

# Doping and temperature dependence of stripes in $p$ -doped lanthanide cuprates

Manfred Bucher

Physics Department, California State University, Fresno,  
Fresno, California 93740-8031

(Dated: May 4, 2020)

## Abstract

Doping  $La_2CuO_4$  with alkaline-earth,  $Ae = Sr, Ba$  (possibly co-doped with lanthanide,  $Ln = Nd, Eu$ ), generates holes in the  $La_{2-y-x}Ln_yAe_xCuO_4$  crystals. A small fraction of the holes,  $\check{p} \leq 0.02$ , suppresses 3D-AFM. The rest resides as *double* holes at  $O$  atoms in the  $CuO_2$  planes. The superlattice, formed by the  $O$  atoms, gives rise to both charge density stripes and magnetization stripes with incommensurability  $q_{c,m}(x) \propto \sqrt{x - \check{p}}$  for  $Ae$  doping up to a watershed value,  $x \leq \hat{x}$ . More doping causes overflow of new holes to the  $LaO$  planes, leaving stripes of *constant*  $q_c$  in the  $CuO_2$  planes. Antiparallel orientation of magnetic moments  $\mathbf{m}(O)$  yields a natural explanation for the coupling of  $q_m(x) = \frac{1}{2}q_c(x)$ . Hole population in the  $LaO$  planes may also be responsible for the watershed in the doping dependence of X-ray intensity, diffracted by stripes, upon cooling through the transition to superconductivity. Above a threshold temperature, electron-hole pairs are thermally generated, but then separate to reside at  $Cu^+$  ions and  $O$  atoms, respectively. The latter, adding to the  $Ae$  generated holes, account for the increase of  $q_c(x, T)$  with temperature. Failing to compensate antiparallel magnetic moments  $\mathbf{m}(Cu^{2+})$ , the thermally generated  $Cu^+$  ions oppose indirectly the magnetic moments of the  $O$  atoms. This breaks the locking of the incommensurability of charge density and magnetization stripes,  $q_m(p) \neq \frac{1}{2}q_c(p)$ . The degree of antiparallel compensation is determined by the relative magnitude of magnetic moments,  $r = |\mathbf{m}(Cu^{2+})| / |\mathbf{m}(O)|$ .

## I. DOPING DEPENDENCE OF STRIPES

Doping  $La_2CuO_4$  with divalent alkaline-earth,  $Ae = Ba, Sr$  (and possibly co-doping with lanthanide  $Ln = Nd, Eu$ ), substitutes ionized lanthanum (and likewise  $Ln$ ) atoms,  $La \rightarrow La^{3+} + 3e^-$ , by ionized  $Ae \rightarrow Ae^{2+} + 2e^-$  in the  $La(Ln)O$  planes of the crystal. This causes locally electron deficiency. For  $Ae$  doping up to a “watershed” value,  $x \leq \hat{x}$ , the missing electron in each substitution is replenished by an electron from an  $O^{2-}$  ion in the  $CuO_2$  plane. There *pairs* of holes neutralize oxygen ions to atoms,  $2e^+ + O^{2-} \rightarrow O$  (to be shown below). Coulomb repulsion spreads the generated double holes (residing in  $O$  atoms) to form a planar superlattice of  $O$  crystal defects. Its periodicity—incommensurate with the crystal lattice and therefore called the “incommensurability”—is given, in reciprocal lattice units (r.l.u.), by

$$q_{c,m}(x)\Big|_{CuO_2} = w_{c,m} \frac{\Omega^\pm}{4} \sqrt{x - \check{p}}, \quad x \leq \hat{x}. \quad (1)$$

The formula is valid for stripes in the  $CuO_2$  planes, as indicated, and for doping below the watershed concentration  $\hat{x}$ , which depends on the species of doping and co-doping. The subscript  $c$  stands for charge density and  $m$  for magnetization. The stripe-kind factor is  $w_c = 2$  or  $w_m = 1$  and the stripe-orientation factor is  $\Omega^+ = \sqrt{2}$  for  $x > x_6 \equiv 2/6^2 \simeq 0.056$  when stripes are parallel to the  $a$  or  $b$  axis, but  $\Omega^- = 1$  for  $x < x_6$  when stripes are diagonal. The offset value  $\check{p} \leq 0.02$  under the radical is the hole concentration necessary to keep three-dimensional antiferromagnetism (3D-AFM) suppressed.

The derivation of Eq. (1) is based on a partition of the  $CuO_2$  plane by pairs of doped holes, incorporating the observed stripe orientation, here in tetragonal approximation of the lattice constants,  $a_0 = b_0$ .<sup>1</sup> Equation (1) is valid at (and near) temperature  $T = 0$ . As no directional preference is used in the derivation, one would expect the corresponding charge density and magnetization pattern to be checkerboard-like rather than stripe-like, as observed. The unidirectional character is imposed by the low-temperature phases of  $La_{2-y-x}Ln_yAe_xCuO_4$  crystals. In these phases  $CuO_6$  octahedra are slightly tilted parallel or diagonally to the planar crystal axes to reduce stress from lattice mismatch, with parallel tilt axes for whole crystal domains. This creates a preference of the charge density and magnetization pattern in one direction over the orthogonal direction, resulting in unidirectional stripes.

A large host of data<sup>5–45</sup> from neutron scattering, hard X-ray diffraction, and soft X-ray resonance spectroscopy is well described by Eq. (1) (see Fig. 1). As mentioned,  $\check{p}$  is the

part of the hole doping necessary to destroy 3D-AFM and keep it suppressed. We may regard these holes as “suppressor holes” (mnemonically indicated by the over-dent of  $\check{p}$ ). Their suppression task keeps them from participating in charge density stripes. For low temperatures and low doping ( $x < 0.09$ ) the offset value agrees with the Néel concentration,  $\check{p} = x_{N0}$ ,

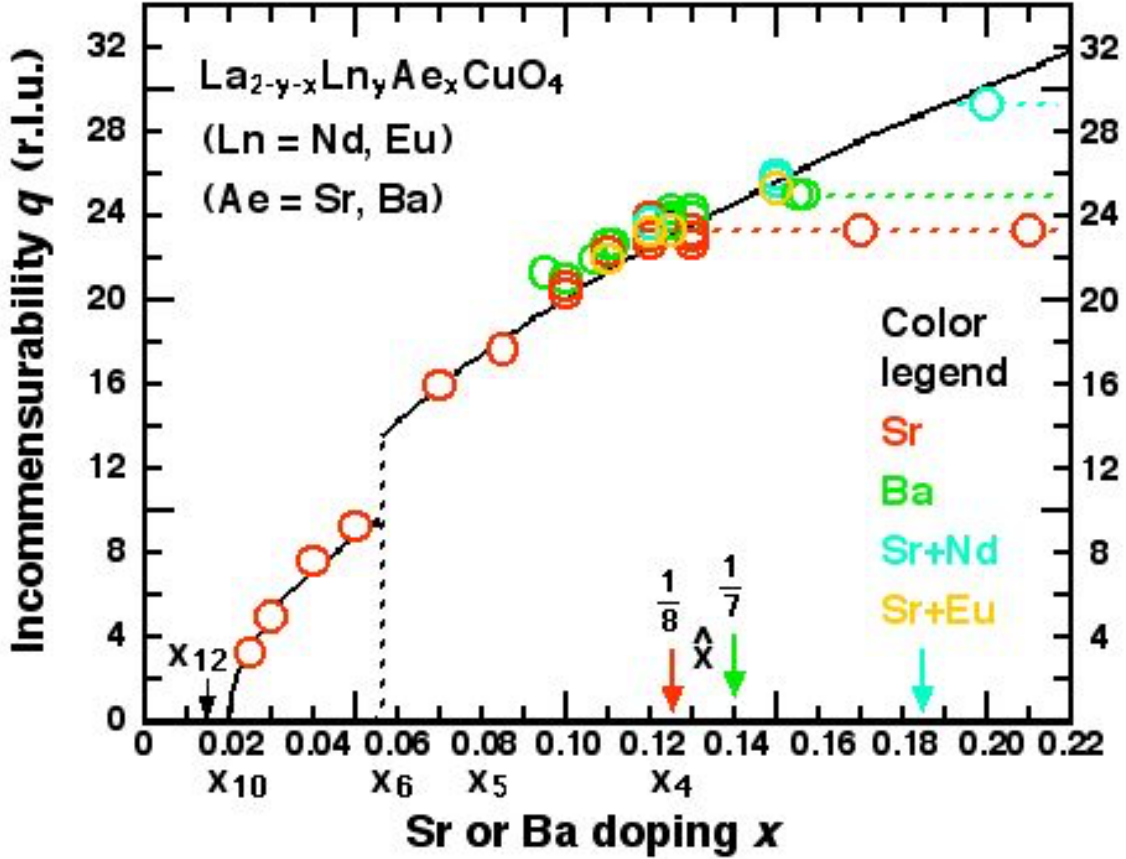


FIG. 1. Incommensurability of charge density stripes,  $q = q_c$ , and of magnetization stripes,  $q = 2q_m$ , in  $La_{2-y-x}Ln_yAe_xCuO_4$  ( $Ln = Nd, Eu$ ) due to doping with  $Ae = Sr$  or  $Ba$ . Circles show data from X-ray diffraction or neutron scattering (Refs. 5 - 45). The broken solid curve is a graph of Eq. (1), calculated with a constant offset value,  $\check{p} = 0.02$ . Commensurate doping concentrations are denoted by  $x_n = 2/n^2$ . The discontinuity at  $x_6 \simeq 0.056$  is caused by a change of stripe orientation, relative to the planar crystal axes, from diagonal for  $x < x_6$  to parallel for  $x > x_6$ . The curve holds for temperature at (and sufficiently near)  $T = 0$  and is accurate for low doping,  $x < 0.09$ . Neglect of the doping dependence of the offset value,  $\check{p}(x) < 0.02$ , causes the slight deviation of the curve (too low) from most data in the doping range  $x > 0.09$ . Doping beyond watershed concentrations,  $\hat{x}_{Sr} = 0.125 = 1/8$ ,  $\hat{x}_{Ba} = 0.14 \simeq 1/7$  and  $\hat{x}_{Sr+Nd} = 0.185$ , yields constant stripe incommensurabilities,  $q_c(x) = 0.235$  ( $Sr$ ),  $0.25$  ( $Ba$ ) and  $0.292$  ( $Sr+Nd$ ), respectively, in agreement with Eq. (2) (dashed horizontal lines).

defined by vanishing Néel temperature,  $T_N(x_{N0}) \equiv 0$ . In  $La_{2-y-x}Ln_yAe_xCuO_4$  compounds it has a value  $x_{N0} = 0.02 = x_{10}$ , marking the collapse of 3D-AFM at  $T = 0$ . With more  $Ae$  doping, but still at  $T \approx 0$ , it is found that a *smaller* value,  $\check{p} < x_{N0}$ , suffices to keep 3D-AFM suppressed.<sup>2</sup> Thus the use of  $\check{p} = 0.02$  in Eq. (1) becomes inaccurate beyond the low doping range,  $x > 0.09$ , as it gives *too small* a value for the incommensurability  $q_{c,m}(x)$ . This can be seen in Fig. 1 where in that range most data points cluster slightly above the drawn  $q(x)$  curve. Use of a *diminished* offset value,  $\check{p} \simeq 0.015$ , in this range shifts that section of the curve slightly upward to better agreement with experiment (not shown). Specifically in the cases of the newly measured data<sup>7-9</sup> from  $La_{1.675}Eu_{0.2}Sr_{0.125}CuO_4$  and  $La_{2-x}Ba_xCuO_4$  ( $x = 0.115, 0.125$ ) at low temperature, the offset values are calculated as  $\check{p} = 0.016, 0.014, 0.015$ , respectively, instead of  $\check{p} = 0.020$  (see Table II, below). What is the reason for the reduction of the offset value (at  $T \approx 0$ ) with more doping? One possibility is that the larger presence of holes in the range  $x < 0.09$ —most of them participating in charge density stripes—assists in keeping 3D-AFM suppressed. It is noteworthy that the diminished offset,  $\check{p} \simeq 0.015$ , is close to  $x_{12} = 0.014$  (see Fig. 1). More may be learned once  $x_{N0} = x_{10} = 0.02$  is theoretically derived.

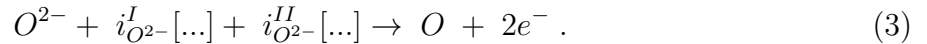
Historically, Eq. (1) was preceded by the empirical, ramp-like “Yamada rule” for magnetization stripes (also called spin density waves), inferred from neutron scattering experiments with  $La_{2-x}Sr_xCuO_4$ .<sup>3</sup> It states that  $q_m = x$  for  $x < 0.12$  but levels off to  $q_m \approx 0.125 = 1/8$  for larger doping. The magnetization stripes were joined by charge density stripes (also called charge density waves) after their discovery in  $La_{1.6-x}Nd_{0.4}Sr_xCuO_4$  by Tranquada *et al.*<sup>4</sup> The two kind of stripes were observed to be related as  $q_c(x) = 2q_m(x)$ . In contrast to the multitude of experimental data for  $x \leq 0.125$ , only a few data had been available until recently for larger doping, with some data falling close to the square-root curve but others considerably below. New data<sup>5-12</sup> from resonant inelastic X-ray spectroscopy (RIXS) of  $La_{2-y-x}Ln_yAe_xCuO_4$  in the doping range  $0.115 \leq x \leq 0.21$  have helped to clarify the situation, amounting to a qualitative change of the incommensurability at watershed doping concentrations  $\hat{x}$  that depend on the doping (and co-doping) species. The qualitative change shows up as *kinks* in the  $q_{c,m}(x)$  profile at  $\hat{x}$ , where the square-root curve from Eq.(1) levels off to constant plateaus,

$$q_c(x)|_{CuO_2} = \frac{\sqrt{2}}{2} \sqrt{\hat{x} - \check{p}}, \quad x > \hat{x}, \quad (2)$$

with values  $\hat{x}_{Sr} = 0.125 = 1/8$ ,  $\hat{x}_{Ba} = 0.14 \simeq 1/7$ , and  $\hat{x}_{Sr+Nd} = 0.185$ . The corresponding constant incommensurabilities are  $q_c(Sr) = 0.235$ ,  $q_c(Ba) = 0.25$ , and  $q_c(Sr+Nd) = 0.292$  (dashed lines in Fig. 1). Although the slope of Yamada’s ramp is only approximately valid, the prediction of a ramp *level* has been confirmed. In order to understand the qualitative change of the incommensurability, we need to take a closer look at the crystal structure.

Figure 2 shows the crystal structure of  $La_2CuO_4$  in hard-sphere ion display. If the ionic charges had to be balanced in each plane of the unit cell, then the  $La^{3+}$  ion in the unit square of a  $LaO$  plane should have one and a half  $O^{2-}$  partners,  $La^{3+}O_{1.5}^{2-}$ , instead of one. By the same token, the  $Cu^{2+}$  ion in the unit square of the  $CuO_2$  plane should then have only one  $O^{2-}$  partner,  $Cu^{2+}O^{2-}$ , instead of two. In reality ionic charge balance is achieved three-dimensionally. For local charge balance one could assign half of an  $O^{2-}$  ion from the unit square of the  $CuO_2$  plane to the unit square of each of the sandwiching  $LaO$  planes,  $La^{3+}O_{1+0.5}^{2-}$ . This leaves for each  $Cu^{2+}$  ion only one  $O^{2-}$  partner,  $Cu^{2+}O_{2-2 \times 0.5}^{2-}$ . The purpose of this consideration is twofold: (i) To show that the  $La^{3+}$  ions (and also their doped  $Ae^{2+}$  substitutes) have some “claim” to some of the  $O^{2-}$  ions in the  $CuO_2$  planes, and (ii) to indicate that electrons in  $O^{2-}$  ions are stronger bound in the  $LaO$  plane than in the  $CuO_2$  plane.

The substitution of a  $La^{3+}$  ion by an  $Ae^{2+}$  ion affects the liberation of the accompanying electron from an  $O^{2-}$  ion in the  $CuO_2$  or  $LaO$  plane as well as the Coulomb repulsion between the holes,  $w(x)$ . Although not stable when free, an  $O^{2-}$  ion is stabilized by the crystal lattice. We express its neutralization in the  $[...] = [CuO_2]$  or  $[LaO]$  plane as



The average ionization energy for liberating an electron from a crystal  $O^{2-}$  ion in the  $[...]$  plane is

$$\bar{i}_{O^{2-}}[...] = \frac{1}{2} \{ i_{O^{2-}}^I[...] + i_{O^{2-}}^{II} [...] \} . \quad (4)$$

As qualitatively argued above—and consistent with the constant incommensurability of stripes in the  $CuO_2$  planes for  $x > \hat{x}$ —the two outer electrons of an  $O^{2-}$  ion are less bound in a virgin (non-hole-doped)  $CuO_2$  plane than in a virgin  $LaO$  plane. It is therefore less costly, in terms of binding energy, to start withdrawing electrons from  $O^{2-}$  ions in the  $CuO_2$  plane instead of from the  $LaO$  plane. However, with each such withdrawal, the density  $x$  of doped holes in the  $CuO_2$  plane (that is, holes per  $a_0 \times b_0$  area of a  $CuO_2$  plaquette), rises.

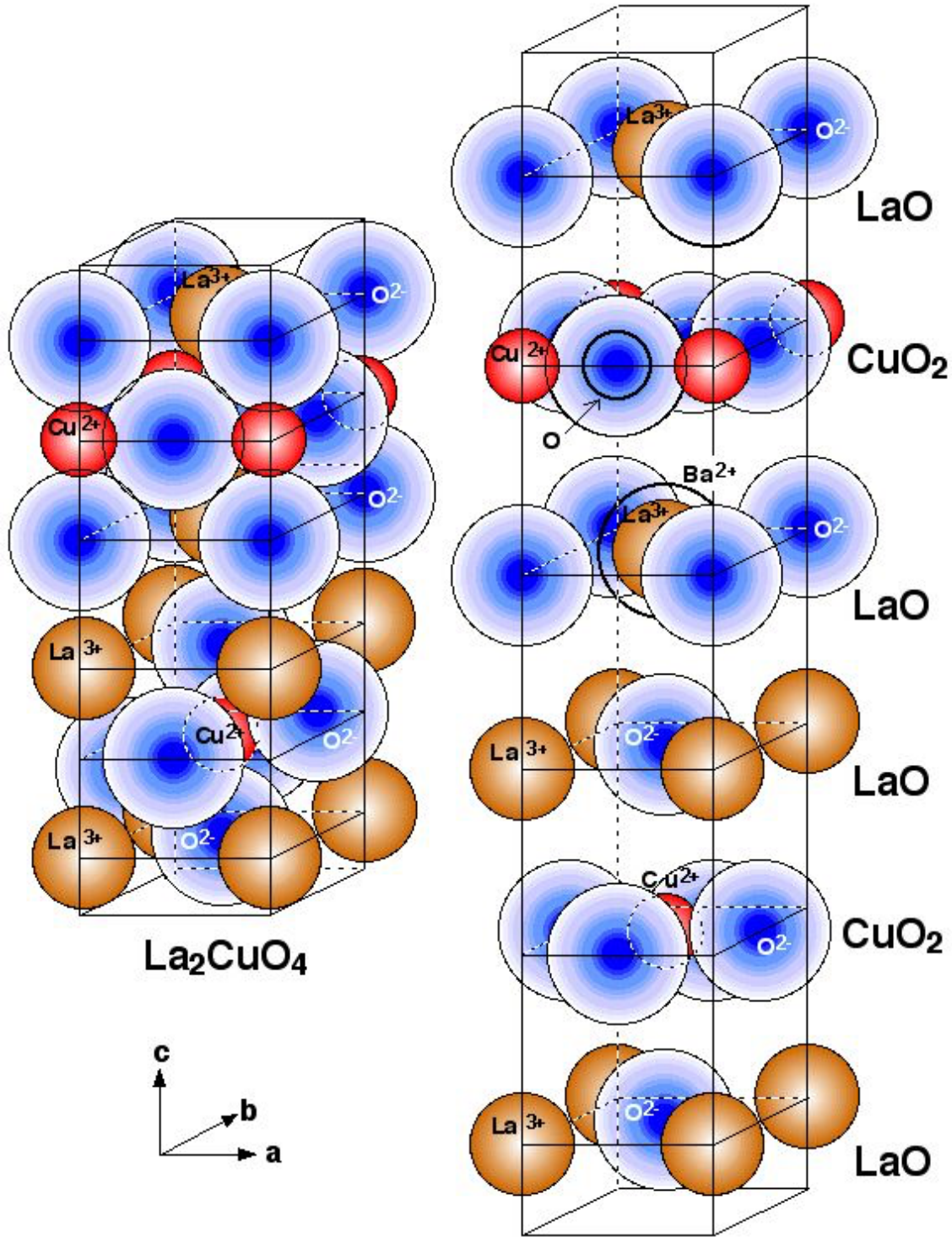


FIG. 2. Double unit cell of  $La_2CuO_4$ , staggered by half the planar lattice constants,  $(\frac{a_0}{2}, \frac{b_0}{2})$ , in hard-sphere ion display (left), and vertically exploded (right) to better show the ion planes as noted on the side. When doped,  $La^{3+}$  ions are substituted by larger-sized  $Sr^{2+}$  or  $Ba^{2+}$ , as illustrated on the right (third plane from the top). Size and position of a lattice-defect  $O$  atom that hosts two holes is also shown (second plane). A  $CuO_6$  octahedron can be seen in the bottom unit cell.

Building up the ensuing charge density,  $\sigma = |e|x$ , in a domain of area  $A$  requires electrostatic work,

$$w(x) = \int^A da \int_0^\sigma \sigma' d\sigma' = C x^2, \quad (5)$$

which makes further withdrawal of electrons from the  $CuO_2$  plane progressively more costly. (The constant  $C$  in Eq. (5) contains the elementary charge  $|e|$  and geometry factors.<sup>46</sup>) The withdrawal of electrons from the hole-doped  $CuO_2$  plane ceases when its cost reaches the cost of withdrawing electrons from the  $LaO$  plane. This happens at watershed doping  $\hat{x}$ ,

$$\bar{i}_{O^{2-}}[CuO_2] + C\hat{x}^2 = \bar{i}_{O^{2-}}[LaO]. \quad (6)$$

Doping beyond the watershed concentration,  $x > \hat{x}$ , will introduce holes to the  $LaO$  planes where they also reside pairwise in  $O$  atoms. Again, Coulomb repulsion spreads the double holes to a superlattice of lattice-defect  $O$  atoms with attending charge density stripes of incommensurability

$$q_c(x)|_{LaO} = \frac{\sqrt{2}}{2} \sqrt{\frac{x - \hat{x}}{2}}, \quad x > \hat{x}. \quad (7)$$

The denominator 2 under the radical accounts for the *two*  $LaO$  planes per unit cell. No offset value  $\check{p}$  occurs in Eq. (7), as suppression of 3D-AFM is already accounted for by Eq. (2). Strictly speaking, there is a slight increase of  $q_c(x)$  in the  $CuO_2$  plane for  $x > \hat{x}$ , over the value from Eq. (2) because of hole-charge density build-up in the  $LaO$  planes. However, it is negligible because of both the  $x^2$  dependence of the Coulomb term in the  $CuO_2$  plane, Eqs. (5, 6), and the *two*  $LaO$  planes per unit cell, Eq. (7).

For the samples that are doped with *Ae only*, a small difference of the watershed concentrations is observed:  $\hat{x}_{Sr} = 0.125 = 1/8$  but  $\hat{x}_{Ba} = 0.14 \simeq 1/7$ . What could be the reason for the difference? Basically, the reason must originate with the different size (ionic radius) of host and doping cations,  $La^{3+} < Sr^{2+} < Ba^{2+}$ . The crystal relieves internal stress from ion-size mismatch by assuming various phases, depending on temperature and doping. The doping dependence of the low-temperature orthorhombic (LTO) and low-temperature tetragonal (LTT) phase,  $0 \leq LTO < x_{LT} < LTT$ , is given by the phase boundary, which is at  $x_{LT} = 0.21$  for *Sr* doping, but in the range  $0.11 < x_{LT} \leq 0.125$  for *Ba* doping (depending on  $T$ ).<sup>43,47,48</sup> The different phases in the doping range of interest—LTO of  $La_{2-x}Sr_xCuO_4$  but LTT of  $La_{2-x}Ba_xCuO_4$ —may account for the different watershed values  $\hat{x}_{Sr}$  and  $\hat{x}_{Ba}$ .

It is known that some properties of lanthanum cuprates extend to higher *Ae* doping when co-doped with *Ln*. A well-known example is the (temperature dependent) doping level  $x^*(T)$

where the pseudogap closes,

$$x_{Ae+Ln}^*(T) = x_{Ae}^*(T) + \Delta x_{Ln}^* , \quad (8)$$

which extends by  $\Delta x_{Ln}^* \approx 0.06$  when co-doped.<sup>30</sup> The extended validity of Eq. (1) for the stripe incommensurability in co-doped samples is in line with that trend:  $\hat{x}_{Sr+Nd} - \hat{x}_{Sr} = 0.185 - 0.125 = 0.06$ .

The close agreement of Eq. (1) with experiment gives credence to the underlying superlattice concept. The spacing of the planar square superlattice,  $L_c(x)$ , is reciprocal to the incommensurability of the charge density stripes,  $L_c(x) = 1/q_c(x)$ . Together with Eq. (1) we obtain the density of the superlattice-forming holes,

$$p - \check{p} = \frac{2}{L_c(x)^2} , \quad (9)$$

as a *pair* of holes per superlattice unit square. In order to localize on the superlattice, *two* holes must reside together on a superlattice site. This leaves as the only viable choice that the defect superlattice is formed by neutral oxygen atoms,  $O^{2-} + 2e^+ \rightarrow O$ .

Below a threshold temperature,  $T < T'$ , the charge density stripes are accompanied by magnetization stripes of incommensurability  $q_m(x) = \frac{1}{2}q_c(x)$ , Eq. (1). What is the mechanism for coupling the incommensurabilities in the ratio of 1:2? The simplest scenario would be that the lattice defects that form the corresponding stripes—be they electric charges, be they magnetic moments—reside at the *same* sites, in this case at  $O$  atoms in the  $CuO_2$  planes, with the *proviso* that the magnetic moments  $\mathbf{m}(O)$  of neighboring  $O$  atoms (with respect to the  $O$  superlattice) are antiparallel. This doubles the spatial period of the magnetization stripes, relative to the charge density stripes, and correspondingly cuts the formers' incommensurability in half. Because of its open shell, a lattice-defect  $O$  atom has a non-vanishing magnetic moment,  $\mathbf{m}(O) \neq 0$ .

## II. WATERSHED FOR STRIPES IN SUPERCONDUCTIVITY

A controversy of long standing has been whether or not stripe order competes with superconductivity. When cooling  $YBa_2Cu_3O_{6+x}$ , the intensity of the X-ray signal from stripe order increases until the transition temperature  $T_c$  to superconductivity is reached, but then *decreases* with more cooling (see Fig. 3).<sup>49,50</sup> This “cooling-curve break” has been

interpreted as a competition between stripe order and superconductivity. The experiment was soon repeated with  $La_{2-x}Sr_xCuO_4$  samples by several research groups, yielding mixed results (see Table I). Recent experiments with  $La_{2-x}Sr_xCuO_4$  show, upon cooling through  $T_c$ , continuing increase of the signal from charge stripes for  $x = 0.115, 0.12, 0.13$  but a *decrease* of the signal for  $x = 0.144, 0.16$ .<sup>10</sup> The new findings present another watershed in the  $Sr$  doping, occurring between  $x = 0.13$  and  $0.144$ . We want to denote the watershed  $Sr$  concentration of the cooling-curve break by  $\hat{X}_{Sr}$ . It is close—but not equal—to the watershed of the compound’s stripe incommensurability,  $\hat{X}_{Sr} \approx \hat{x}_{Sr} = 0.125$ .

A clear increase of the cooling curve below  $T_c$  was also found for  $La_{2-x}Ba_xCuO_4$  with  $Ba$  doping  $x = 0.095$  and  $0.11$  (see Table I).<sup>43</sup> The flat cooling curves for the doping values that flank the  $Ba$  concentration  $x = 0.125 = 1/8$ —that is,  $x = 0.115$  and  $0.135$ —may be affected by the so-called “1/8 anomaly” where superconductivity is strongly suppressed,  $T_c(1/8) \simeq 3$  K. If the measurement of the  $x = 0.155$  doped crystal has validity (despite its low statistical significance), it would indicate a cooling-curve watershed in  $La_{2-x}Ba_xCuO_4$  in the range  $0.135 < \hat{X}_{Ba} < 0.155$ , in good coincidence with the stripe watershed  $\hat{x}_{Ba} = 0.14$ . It seems therefore warranted to explore whether a common cause exists, and more specifically, whether  $\hat{X} = \hat{x}$ ?

It is observed that the cooling does *not* affect the incommensurability of the stripes. By Eqs. (1, 2) this means that the cooling does not affect the density  $x - \check{p}$  or  $\hat{x} - \check{p}$  of stripe-forming holes in the  $CuO_2$  planes. The change of X-ray intensity must therefore be due to fluctuations of the  $O$  superlattice that degrade the diffraction in terms of lesser correlation lengths. Instead of cooling down from  $T_c \rightarrow 0$ , as in experiment, the cooling curves are

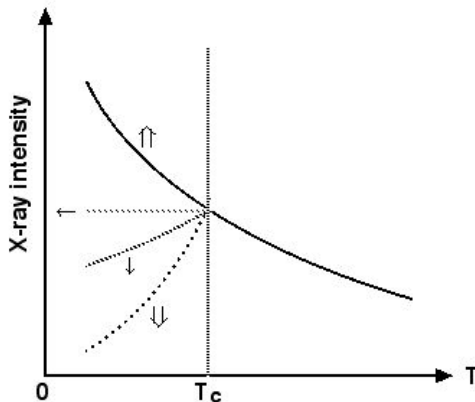


FIG. 3. Cooling curves (schematically) of X-ray intensity diffracted by charge density stripes in the  $CuO_2$  planes of  $La_{2-x}Ae_xCuO_4$  ( $Ae = Sr, Ba$ ). The arrows correspond with Table I.

easier understood for the reverse process of *warming* up from  $T = 0 \rightarrow T_c$ . In this case, increasing thermal fluctuations with rising temperature lead to steadily decreasing signal strength, with no break when passing through  $T_c$ . Turning to the other case, an increasing

| Dop-ant | $x$<br>nominal | $q_c$<br>[r.l.u.]    | cooling<br>curve $< T_c$ | Ref. | Year | Comment                                    |
|---------|----------------|----------------------|--------------------------|------|------|--|
| Sr      | <b>0.12</b>    | 0.24*                | ↑                        | 51   | 2012 | *only surface stripes                      |
| Sr      | 0.110          | 0.224                | ↓                        | 30   | 2014 |  |
| Sr      | <b>0.120</b>   | 0.235                | ↓                        | 30   | 2014 |  |
| Sr      | 0.130          | 0.232                | ↓                        | 30   | 2014 |  |
| Sr      | <b>0.12</b>    | 0.236 <sup>†</sup>   | ↓                        | 20   | 2014 | <sup>†</sup> rotated 2.7° in the plane     |
| Sr      | <b>0.12</b>    | 0.231                | ←                        | 21   | 2014 |  |
| Sr      | <b>0.12</b>    | 0.24(6) <sup>‡</sup> | not probed               | 6    | 2017 | <sup>‡</sup> included for $q_c$ comparison |
| Sr      | 0.115          | 0.226                | ↑                        | 10   | 2019 |  |
| Sr      | <b>0.12</b>    | 0.2264               | ↑                        | 10   | 2019 |  |
| Sr      | 0.13           | 0.2281               | ↑                        | 10   | 2019 |  |
| Sr      | 0.144          | 0.2321               | ↓                        | 10   | 2019 |  |
| Sr      | 0.16           | 0.2322               | ↓                        | 10   | 2019 |  |
| Sr      | <b>0.12</b>    | 0.232 <sup>‡</sup>   | not probed               | 12   | 2020 | <sup>‡</sup> included for $q_c$ comparison |
| Ba      | 0.095          | 0.205                | ↑                        | 43   | 2011 |  |
| Ba      | 0.110          | 0.219                | ↑                        | 43   | 2011 |  |
| Ba      | 0.115          | 0.228                | ←                        | 43   | 2011 |  |
| Ba      | <i>0.125</i>   | 0.232                | $> T_c$                  | 43   | 2011 |  |
| Ba      | 0.135          | 0.243                | ←                        | 43   | 2011 |  |
| Ba      | 0.155          | 0.245                | ↓ <sup>§</sup>           | 43   | 2011 | <sup>§</sup> low statistics                |

TABLE I: Trend of the cooling curves of the X-ray intensity diffracted by charge density stripes with incommensurability  $q_c(x)$  in  $La_{2-x}Ae_xCuO_4$  ( $Ae = Sr, Ba$ ) below the transition temperature  $T_c$  (except for  $La_{1.875}Ba_{0.125}CuO_4$ ). Double up-arrows and down-arrows signify clear increase and decrease, respectively. Single down-arrows signify moderate decrease and left-arrows indicate flat cooling curves. Cases with  $x = 0.12$  are marked bold for ease of comparison.

warming curve—or decreasing cooling curve—is, besides  $T < T_c$ , subject to the condition  $x > \hat{X}_{Ae}$ . If the curve break is caused by the stripe watershed,  $\hat{X}_{Ae} = \hat{x}_{Ae}$ , then the switch of double-hole residence from  $O$  atoms in the  $CuO_2$  plane to  $O$  atoms in the  $LaO$  plane becomes relevant.

In order to deal with the superconducting phase we need to make assumptions about superconductivity in  $La_{2-x}Ae_xCuO_4$ . As a model, we want to assume that the superconducting state makes possible a scatterfree transfer of double holes back and forth between lattice defect  $O$  atoms and their immediate  $O^{2-}$  neighbor ions. At  $Ae$  doping below the watershed,  $x < \hat{x}$ , the  $O$  atom and the closest  $O^{2-}$  neighbors assessible to the double holes are in the  $CuO_2$  plane, located at face positions of the unit-square (see Fig. 2). At all temperatures, Coulomb repulsion tends to keep the double holes on their superlattice site, facilitated by close superconducting fluctuations. However, with increasing temperature, thermal agitation of lattice ions gives rise to larger fluctuations that degrade X-ray diffraction, diminishing their intensity. The result is a steadily decreasing warming curve—or increasing cooling curve—unimpeded by passing  $T_c$ .

With  $Ae$  doping at and beyond the watershed,  $x \geq \hat{x}$ , the chemical potential of  $O$  atoms in the  $CuO_2$  plane and in the  $LaO$  plane is equal. Now superconducting double holes can also fluctuate between an  $O$  atom at a superlattice site in the  $CuO_2$  plane and either one of the four  $O^{2-}$  neighbors, located in the sandwiching  $LaO$  planes as well as on the same unit-cell face (see Fig. 2). For example, if the  $O$  atom is at a superlattice site  $(\frac{1}{2}, 0, \frac{1}{2})$ , then those  $O^{2-}$  ions are at positions  $(\frac{1}{2} \pm \frac{1}{2}, 0, \frac{1}{2} \pm \frac{1}{2})$ . Such fluctuations considerably reduce the average presence of  $O$  atoms in the  $CuO_2$  planes and thus the intensity of the diffracted X-rays from the  $CuO_2$  planes. The fluctuating presence of  $O$  atoms in the  $CuO_2$  planes does not change the stripe incommensurability  $q_c$  because the superlattice spacing persists—the close fluctuation displacements to the sandwiching  $LaO$  planes are negligible with respect to the superlattice spacing. The described effect is largest at  $T = 0$  but decreases to termination with  $T \rightarrow T_c$  because of diminishing super/normal-conducting phase ratio (Gortner-Kasimir two-phase model of superconductivity). The result is a steadily increasing warming curve up to  $T_c$ —or decreasing cooling curve down from  $T_c$ —where it joins the curve that is affected only by thermal fluctuations.

As Table I shows, the  $q_c(x)$  values measured by different researchers are close, but minor differences persist. This can be seen best in a comparison of the data for  $x = 0.12$  (bold

print). The disagreements may be due to differences in crystal growth, measurement equipment, data processing or background removal. Uncertainties are amplified when it comes to the trend of the cooling curves, and thus to the watershed doping  $\hat{X}$ . This may explain the different trends near  $Sr$  doping  $x = 0.125$  that have been observed by different researchers. It is therefore valuable to have cooling curves for  $Ae$  doping  $x$  distinctly away from the watershed  $\hat{X}$ . The series of cooling curves measured by Wen *et al.*<sup>10</sup> for  $0.115 \leq x \leq 0.16$  shows a qualitative change in the curve profile with  $Sr$  doping. Leaving the measurement for  $x = 0.13$  temporarily aside (because of a re-calibration), the watershed value must lie in the doping interval  $0.12 < \hat{X}_{Sr} < 0.144$ . When the  $La_{2-x}Sr_xCuO_4$  crystal with nominal doping  $x = 0.13$  is re-calibrated (see Appendix A), an effective doping value  $x_{Sr}^{eff} = 0.121 < 0.125$  is obtained. This opens the possibility of a common origin for the watersheds in stripe pattern and cooling curves,  $\hat{X}_{Sr} \simeq \hat{x}_{Sr} = 1/8$ .

What can be learned about stripe-superconductivity competition? Such competition was inferred from *decreasing* cooling curves. There seems to be now sufficient evidence, that *no* decreasing cooling curves are observed for  $Ae$  doping  $x < \hat{X} \simeq \hat{x}$ . Their observation for  $x > \hat{X} \simeq \hat{x}$  may be attributed to superconducting fluctuations of double holes in  $O$  atoms of both the  $CuO_2$  and  $LaO$  planes, as the present study proposes.

Another indication for stripe-superconductivity competition has been seen in the  $1/8$  anomaly of  $La_{1.85}Ba_{0.125}CuO_4$ , that is, the sudden drop of  $T_c$  to 3 K. The attribution to charge density stripes has been rationalized by the maximum of the charge-density and magnetization stripe observation temperature,  $T_{cdw}(x)$  and  $T_{sdw}(x)$ , near  $x = 0.125$ .<sup>43</sup> However, it should be pointed out that the incommensurability of the stripes *at*  $x = 0.125$ ,  $q_c(0.125|Ba) \simeq 0.235$  and  $q_m(0.125|Ba) \simeq 0.117$ , is *not* 1:4 or 1:8 commensurate with the crystal. It is not obvious why these incommensurate stripes would suppress superconductivity at  $x = 0.125$ .

More persuasive is an indication for stripe-superconductivity competition in the  $Sr$  doped compound,  $La_{2-x}Sr_xCuO_4$ , where the  $T_{cdw}(x)$  and  $T_{sdw}(x)$  domes, centered near  $x = 0.125$ ,<sup>10,30,52</sup> coincide with the doping range of a big dent in the otherwise parabolic  $T_c(x)$  dome. But  $x < 0.125$  is the doping range with rising cooling curves, which show *no* competition—the dent must have a different origin.

Another argument is based on an enhancement of diffracted X-ray intensity from stripes when superconductivity is destroyed with a strong magnetic field, first observed

in  $YBa_2Cu_3O_{6.67}$ .<sup>49,50</sup> It is interpreted as suppression of stripes by superconductivity. The problem with this reasoning is that the introduction of another variable—the magnetic field—prevents a mono-causal conclusion. The experiment was repeated for the same series of  $La_{2-x}Ba_xCuO_4$  crystals where previously cooling curves without a magnetic field had been observed.<sup>53</sup> The findings show that field enhancement is *relatively* large at  $Ba$  doping  $x = 0.125 \pm 0.03$ , that is, where the stripe intensity is weak, but much smaller near  $x = 0.125$  where stripe intensity is strong. The field effect is most pronounced at very low temperature ( $T = 3K$ ) but fades rapidly with increasing temperature—much faster than the thermal decrease of stripe intensity without a field. A possible explanation of the findings could be that the field enhancement is caused by a slight upgrade of the diffraction condition of the  $O$  superlattice, stiffened through stabilization of its magnetic moments  $\mathbf{m}(O)$  by a gain of Zeeman energy in the field.<sup>53</sup> It is a small energy gain, essentially independent of doping  $x$ , but increasing with field strength, and quickly overcome by thermal agitation with rising temperature. A view at the experimental spectra<sup>53</sup> indicates that the *absolute* field enhancement is comparable in the samples of the probed doping range,  $0.095 \leq x \leq 0.155$ , which would corroborate this interpretation. Rather than compete with stripes, superconductivity passively stands by as thermal fluctuations eat away at stripe diffractibility.

Taken together, the counter-arguments leave little support for the notion of stripe-superconductivity competition.

### III. TEMPERATURE DEPENDENCE OF STRIPES

Three of the recent articles also address the temperature dependence of charge density stripes in  $La_{2-x}Ba_xCuO_4$  ( $x = 0.115, 0.125, 1.555$ ) and  $La_{1.675}Eu_{0.2}Sr_{0.125}CuO_4$ .<sup>7-9</sup> Three aspects among the new experimental findings are:

#1 The incommensurability of charge density stripes is essentially constant up to a threshold temperature  $T'$ ,

$$q_c(x, T \leq T') \simeq q_c(x|T = 0) , \quad (10)$$

as given by Eqs. (1, 2), but then increases linearly at higher temperatures,

$$q_c(x, T > T') = q_c(x, T \leq T') + c \times (T - T') , \quad (11)$$

with a compound specific thermal coefficient  $c > 0$  (depending slightly on doping  $x$ ).<sup>7-9</sup>

#2 An exception is seen in the strontium-doped cuprate,  $La_{1.675}Eu_{0.2}Sr_{0.125}CuO_4$ , below the threshold temperature,  $T < T'$ , where increasing temperature causes a slight *decrease* of the incommensurability.<sup>9</sup>

#3 In the barium-doped cuprate  $La_{1.875}Ba_{0.125}CuO_4$ , the rigid coupling of the incommensurability of charge density stripes and magnetization stripes,  $q_c(x) = 2q_m(x)$ , Eq. (1), ceases above the threshold temperature,  $T > T'$ . Whereas the incommensurability of the charge density stripes keeps increasing with temperature, Eq. (11), the (double) incommensurability of the *magnetization* stripes *decreases* by about the same rate,<sup>7</sup>

$$2q_m(x, T > T') = 2q_m(x, T \leq T') - c \times (T - T') . \quad (12)$$

#### IV. EXPLANATION OF EXPERIMENTAL FINDING #2

In the attempt to explain these experimental findings we start with the second aspect—the slight *decrease* of  $q_c(T)$  with increasing temperature in  $La_{1.675}Eu_{0.2}Sr_{0.125}CuO_4$  below the threshold temperature,  $T < T'$ . This appears as an exception to the general trend of constant incommensurability below  $T'$ , but of increasing values above, Eqs. (10, 11). The key of this “exception” lies in the offset hole concentration  $\check{p}$  which appears under the radical in Eq. (1). While the presence of stripe-forming holes in the range  $x > 0.09$  assists in keeping 3D-AFM suppressed, such assistance seems to cease with higher mobility of crystal constituents at elevated temperatures. In that case the offset must approach the full value of the *temperature-dependent* Néel concentration,  $\check{p} \rightarrow x_N(T)$ . This can be seen in the case of  $La_{1.675}Eu_{0.2}Sr_{0.125}CuO_4$ , listed at the top of Table II: At low temperature,  $T = 25$  K, the offset value is clearly less than the Néel concentration,  $\check{p} = 0.016 < 0.020 = x_{N0}$ , but at elevated temperature,  $T' = 80$  K, the offset is calculated to be very close to the Néel concentration,  $\check{p}(80\text{K}) = 0.020 \simeq x_N(80\text{K}) = 0.019$ . (The comparison here is with  $x_N(T')$  of  $La_{2-x}Ae_xCuO_4$ —co-doping with  $Eu$  could slightly change its value.) The approach of  $\check{p} = 0.016 \rightarrow 0.020$  with increasing temperature below  $T'$  is reflected in a slightly downward parabolic arc of the  $q_c(T)$  display for  $T = 25$  K  $\rightarrow$  80 K =  $T'$  (Fig. 3a in Ref. 9), caused by the square-root dependence in Eq. (1).

## V. EXPLANATION OF EXPERIMENTAL FINDING #1

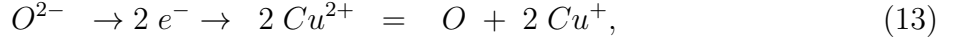
If the charge density stripes are caused by the doped holes and if Eq. (1) adequately gives their incommensurability  $q_c(p)$ , then the observed  $q_c$  value, together with the temperature-dependent Néel concentration for the offset value  $\check{p} = x_N(T)$ , can be used to calculate the hole density  $p(T)$  at elevated temperatures. For  $La_{1.675}Eu_{0.2}Sr_{0.125}CuO_4$  at  $T = 210$  K this gives a hole concentration of  $p(T_{210K}) = 0.152 > x = 0.125$ , considerably larger than the  $Sr$  doping (see Table II). Similarly, for  $La_{2-x}Ba_xCuO_4$  ( $x = 0.115, 0.125$ ) at  $T = 49$  K and 90 K, this gives hole concentrations of  $p(T_{49K}) = 0.130 > 0.115$  and  $p(T_{90K}) = 0.167 > 0.125$ .

Where do the additional holes come from? We may regard them as “thermally generated holes.” More specifically, they can be regarded as the positive electric partners of thermally generated electron-hole *pairs*, required by charge neutrality of the crystal. A possible

| $T$ [K] | $T'$ [K] | Compound                      | $x$   | $p(T)$       | $\Delta p$ | $q_c$ [r.l.u.] | $x_N(T)$ | $\check{p}$  | Ref. |
|---------|----------|-------------------------------|-------|--------------|------------|----------------|----------|--------------|------|
| 25      | 80       | $La_{1.8-x}Eu_{0.2}Sr_xCuO_4$ | 0.125 | =0.125       |            | 0.233          | 0.020    | <b>0.016</b> | 9    |
| 80      | 80       | $La_{1.8-x}Eu_{0.2}Sr_xCuO_4$ | 0.125 | =0.125       |            | 0.229          | 0.019    | <b>0.020</b> | 9    |
| 210     | 80       | $La_{1.8-x}Eu_{0.2}Sr_xCuO_4$ | 0.125 | <b>0.152</b> | 0.027      | 0.27           | 0.006    | =0.006       | 9    |
| 20      | 33       | $La_{2-x}Ba_xCuO_4$           | 0.115 | =0.115       |            | 0.225          | 0.020    | <b>0.014</b> | 8    |
| 33      | 33       | $La_{2-x}Ba_xCuO_4$           | 0.115 | =0.115       |            | 0.225          | 0.020    | <b>0.014</b> | 8    |
| 49      | 33       | $La_{2-x}Ba_xCuO_4$           | 0.115 | <b>0.130</b> | 0.015      | 0.240          | 0.020    | 0.015*       | 8    |
|         |          |                               |       |              |            |                |          | *estimate    |      |
| 23      | 54       | $La_{2-x}Ba_xCuO_4$           | 0.125 | =0.125       |            | 0.235          | 0.020    | <b>0.015</b> | 7,8  |
| 54      | 54       | $La_{2-x}Ba_xCuO_4$           | 0.125 | =0.125       |            | 0.235          | 0.020    | <b>0.015</b> | 7,8  |
| 90      | 54       | $La_{2-x}Ba_xCuO_4$           | 0.125 | <b>0.167</b> | 0.042      | 0.272          | 0.019    | =0.019       | 7,8  |

TABLE II: Incommensurability  $q_c$  of charge density stripes in lanthanide cuprates, measured with RIXS at temperature  $T$  by the referenced authors. Crystals are doped with  $Sr$  or  $Ba$  in nominal concentration  $x$ . The threshold temperature  $T'$  denotes the onset of temperature-dependent increase of  $q_c$ . Experimental values of the Néel concentration  $x_N(T)$  are from Ref. 54. The hole concentration  $p(T)$  and the offset value  $\check{p}$  are assumed to be equal to the preceding entry, indicated by the '=' sign, but otherwise **calculated** (bold print) with Eq. (16). The values in the  $\Delta p$  column give the concentration of thermally generated holes,  $\Delta p = p^\dagger(T)$ .

scenario could be a thermally activated transfer of electrons (here symbolized by  $\rightarrow e^- \rightarrow$ ) from crystal  $O^{2-}$  ions to crystal  $Cu^{2+}$  ions,



leaving  $O$  atoms and twice the amount of  $Cu^+$  ions as lattice defects behind. The latter ions would harbor the thermally generated electrons of concentration

$$n^\dagger(T) = p^\dagger(T), \quad T > T'. \quad (14)$$

Adding the thermally generated holes to the holes introduced by  $Ae$  doping yields the total hole concentration,

$$p(T) = x + p^\dagger(T). \quad (15)$$

It gives rise to the observed charge density stripes of incommensurability,

$$q_c(x, T > T') \Big|_{CuO_2} = \frac{\Omega^\pm}{2} \sqrt{p(T) - \check{p}} = q_c(x, T \leq T') + c \times (T - T'), \quad (16)$$

with  $c = (\Omega^\pm)^2 \frac{dp^\dagger}{dT} \Big|_{T'} / q_c(x, T \leq T')$ , obtained by Taylor expansion.

What happens to the thermally generated *electrons*? Hosted by  $Cu^+$  ions, we assume that they spread out to form a lattice defect  $Cu^+$  superlattice and corresponding charge density stripes with incommensurability

$$q_c(n^\dagger) \Big|_{CuO_2} = \frac{\Omega^\pm}{\sqrt{2}} \sqrt{n^\dagger}. \quad (17)$$

The stripe-orientation factors are  $\Omega^+ = \sqrt{2}$  and  $\Omega^- = 1$  for parallel or diagonal stripes, as in Eq. (1). The formula accounts for *one* thermally generated electron per  $Cu^+$  ion, in contrast to Eq. (1) which accounts for two doped holes per  $O$  atom. No setoff  $\check{p}$  appears under the radical in Eq. (17)—no 3D-AFM suppression by electrons. Detecting charge density stripes from the  $Cu^+$  superlattice poses a new challenge to experimenters. The accompanying magnetization stripes cannot be observed by themselves, since they combine with those from the  $O$  superlattice, as explained next.

## VI. EXPLANATION OF EXPERIMENTAL FINDING #3

Above the threshold temperature  $T'$  we assume that thermally activated electron-hole pairs are generated, which then separate and reside at  $Cu^+$  and  $O$  lattice defects, respectively, Eq. (13). The *increase* of the charge density stripes' incommensurability with temperature, Eq. (11), has been interpreted in Sect. V through an increase of hole concentration,

Eq. (15). We now turn our attention to the magnetic moments of the crystal defects. Antiferromagnetism in the  $CuO_2$  planes of the  $La_2CuO_4$  host is achieved by antiparallel orientation of neighboring magnetic moments  $\mathbf{m}(Cu^{2+})$ . The closed-shell oxygen ions provide no contribution to AFM in the host,  $\mathbf{m}(O^{2-}) = 0$ . However, the magnetic moments  $\mathbf{m}(O) \neq 0$  of the  $O$  atoms, generated by  $Ae$  doping and distributed both incommensurably and antiparallel, give rise to the magnetization stripes that are detected below the threshold temperature  $T'$ . At temperatures  $T > T'$ , more  $\mathbf{m}(O)$  moments are *thermally* generated, but also twice the amount of  $\mathbf{m}(Cu^+) = 0$  moments of (closed-shell)  $Cu^+$  defects, Eq. (13). The former moments add to the concentration of  $\mathbf{m}(O)$  moments, the latter affect it indirectly: By replacing a  $Cu^{2+}$  lattice ion, each thermally generated  $Cu^+$  ion eliminates a  $\mathbf{m}(Cu^{2+}) \neq 0$  moment that previously had been compensating the antiparallel  $\mathbf{m}(Cu^{2+})$  moment of its  $Cu^{2+}$  neighbor. It is thus the  $\mathbf{m}(Cu^{2+})$  moments of those *uncompensated*  $Cu^{2+}$  neighbors that now compensate some of the  $\mathbf{m}(O)$  moments, generated by both  $Ae$  doping and thermal activation. The result of thermal activation above  $T'$  is therefore an increase of the concentration of  $\mathbf{m}(O)$  moments by  $p^\dagger/2$  due to thermally generated  $\mathbf{m}(O)$  moments, but also a decrease of their magnetization, caused indirectly by thermally generated  $\mathbf{m}(Cu^+)$  moments by  $n^\dagger$  (in terms of uncompensated  $\mathbf{m}(Cu^{2+})$  moments). Whether there is a *net* increase or decrease of the total  $\mathbf{m}(O)$  magnetization—and accordingly of the incommensurability  $q_m$  of the magnetization stripes—depends on the relative magnitude of  $\mathbf{m}(Cu^{2+})$  and  $\mathbf{m}(O)$ ,

$$r = \frac{|\mathbf{m}(Cu^{2+})|}{|\mathbf{m}(O)|}. \quad (18)$$

For example, if we had  $r = 1$ , then each  $\mathbf{m}(Cu^{2+})$  moment would compensate one antiparallel  $\mathbf{m}(O)$  moment. In general, each  $\mathbf{m}(Cu^{2+})$  moment compensates (on average)  $r$   $\mathbf{m}(O)$  moments. By Eqs. (13-16, 1) the remaining concentration of uncompensated  $\mathbf{m}(O)$  moments,

$$[\mathbf{m}(O)] \equiv \frac{x - \check{p}}{2} + \frac{p^\dagger}{2} - n^\dagger = \frac{x - \check{p}}{2} + \frac{1 - 2r}{2} p^\dagger, \quad (19)$$

gives rise to a magnetic stripe incommensurability

$$2q_m(x, T > T') = 2 \frac{\Omega^\pm}{4} \sqrt{x - \check{p} + (1 - 2r)p^\dagger} = 2q_m(x, T \leq T') + (1 - 2r)c \times (T - T'). \quad (20)$$

Comparison with the temperature dependence of charge density stripes, Eq. (16), shows that for  $r = 1$  the (double) incommensurability of magnetic stripes would *decrease* with increasing

temperature by a rate comparable with the increase of the incommensurability of the charge density stripes. Experimental values of  $|\mathbf{m}(Cu^{2+})|$  in  $La_2CuO_4$  and  $YBa_2Cu_3O_{6+y}$  vary somewhat, but  $|\mathbf{m}(Cu^+)| \approx 0.6\mu_B$  (in Bohr magneton unit) is regarded as most likely.<sup>55-60</sup> What is missing for a validation of the present scenario, Eqs. (18, 20), is a value of  $|\mathbf{m}(O)|$ .

## VII. CONCLUSION

Doping  $La_2CuO_4$  with alkaline-earth,  $Ae = Sr, Ba$ , (and possibly co-doping with lanthanide  $Ln = Nd, Eu$ ) generates holes in the  $La_{2-y-x}Ln_yAe_xCuO_4$  crystals. A small fraction of the holes,  $\check{p} \leq 0.02$ , is itinerant and actively suppresses 3D-AFM. The remaining holes, of concentration  $x - \check{p}$ , reside as double holes at  $O$  atoms. The superlattice formed by the  $O$  atoms gives rise to both charge density stripes and magnetization stripes with incommensurability  $q_{c,m}(x) \propto \sqrt{x - \check{p}}$ . The setoff value  $\check{p}$  depends on the doping level and on temperature. Near  $T = 0$  its value is  $\check{p} = x_{N0} = 0.02 = x_{10}$  for low doping,  $x < 0.09$ , but less,  $\check{p} \approx 0.015$ , in the doping range above. However, with increasing temperature the setoff value approaches the Néel concentration,  $\check{p} \rightarrow x_N(T)$ , at any doping level  $x$ . With respect to the  $O$  superlattice, the antiparallel orientation of neighboring magnetic moments  $\mathbf{m}(O)$  yields a natural explanation for the coupling of  $q_m(x) = \frac{1}{2}q_c(x)$ , valid below the threshold of temperature dependence,  $T < T'$ . Increasing density of the doped holes, hosted pairwise in the  $CuO_2$  planes in lattice defect  $O$  atoms, raises their chemical potential. When doping exceeds a watershed value,  $x > \hat{x}$ , additional holes overflow to the  $LaO$  planes where they also reside pairwise in  $O$  atoms. This leaves charge density stripes of constant  $q_c$  in the  $CuO_2$  planes. The watershed concentration of the stripes' incommensurability, due to commencing hole population in the  $LaO$  planes, may also cause a watershed division of the cooling curves of the intensity of X-rays, diffracted by stripes, when the crystals are cooled below the superconducting transition,  $T < T_c$ .

Above the threshold temperature,  $T > T'$ , electron-hole pairs are thermally generated. They separate to reside at  $Cu^+$  ions and  $O$  atoms, respectively. The latter, adding to the  $Ae$  generated holes, account for the increase of the incommensurability of charge density stripes with temperature. The concentration of the magnetic moments of thermally generated  $Cu^+$  ions affect indirectly (in terms of antiparallel compensation) the concentration of the magnetic moments of the  $O$  atoms. As a consequence, the locking of the incommensurability

of charge density stripes and magnetization stripes then no longer holds,  $q_m(x) \neq \frac{1}{2}q_c(x)$ . The degree of antiparallel compensation is determined by the relative magnitude of magnetic moments,  $r = |\mathbf{m}(Cu^{2+})| / |\mathbf{m}(O)|$ . If  $|\mathbf{m}(O)| \approx |\mathbf{m}(Cu^{2+})|$  can be found, then this would explain the observed *decrease* of  $2q_m(p, T)$  by about the same rate as the increase of  $q_c(p, T)$ .

### Appendix A: RECALIBRATION OF A DOPING VALUE

In the series of stripe incommensurabilities of  $La_{2-x}Sr_xCuO_4$ , measured by Wen *et al.*,<sup>10</sup> the value for nominal  $Sr$  doping  $x = 0.13$ ,  $q_c = 0.2281$ , is considerably smaller than  $q_c(x) = 0.235$ , obtained from Eq. (2) for  $x \geq 0.125$ . Therefore a recalibration to an effective, stripe-generating concentration  $x^{eff}$  is carried out with the following procedure: Data from the doping range where stripe incommensurability is constant,  $q_c(x) = 0.235$ ,  $x > 0.125$ , are used from the series under consideration<sup>10</sup> and from a control group<sup>12</sup> in order to obtain with Eq. (2) the corresponding offset value  $\check{p}$ . The  $\check{p}$  value is then used to calculate with

| Ref. | $T$ [K] | $x$<br>nominal | $q_c$ expt.<br>[r.l.u.] | $q_c$ calculated with<br>Eq. (1) and $\check{p} = 0.013$ | $q_c$ calculated with<br>Eq. (1) and $\check{p} = 0.017$ |
|------|---------|----------------|-------------------------|--|--|
| 10   | 23.3    | 0.115          | 0.226                   | ← ← ← ← ←  | 0.221 almost agreement                                   |
| 10   | 28.4    | 0.12           | 0.2264                  | ← ← ← ← ← ←  | <b>0.227</b> close agreement                             |
| 12   | 40      | 0.12           | 0.232                   | <b>0.232</b> full agreement                              |  |
| 10   | 30.8    | 0.13           | <i>0.2281</i>           | ← used to recalibrate                                    | with $\check{p} = 0.017$                                 |
| 10   | 37.5    | 0.144          | 0.2321                  |  | <u>0.23215</u> used in Eq. (2)                           |
| 10   | 35.5    | 0.16           | 0.2322                  |  | <u>0.23215</u> to obtain $\check{p} \uparrow$            |
| 12   | 40      | 0.17           | 0.236                   | <u>0.237</u> used in Eq. (2)                             |  |
| 12   | 40      | 0.21           | 0.238                   | <u>0.237</u> to obtain $\check{p} \uparrow$              |  |

TABLE III: Incommensurability  $q_c(x)$  of  $La_{2-x}Sr_xCuO_4$  at temperature  $T$ , nominally doped with  $Sr$  concentration  $x$ . From each research group the average experimental value in the  $0.144 \leq x \leq 0.21$  doping range of constant  $q_c$  is used (overlined in the bottom part of the table) to obtain offset values  $\check{p}$  for calculating  $q_c$  at  $x \leq 0.12$ . It yields agreement (bold print) or almost agreement with experiment (top part of the table). With  $\check{p} = 0.017$  and  $q_c = 0.2281$  an effective, stripe-generating  $Sr$  doping is calculated,  $x^{eff} = 0.121$ , instead of nominal  $x = 0.13$  (center line).

Eq. (1)  $q_c(x)$  for  $x \leq 0.12$ . The results are in close agreement with the experimental values (see Table III), which validates the procedure. The setoff  $\check{p} = 0.017$  and the experimental  $q_c(0.13) = 0.2281$  are then used to calculate with Eq. (1) an effective, stripe-generating  $Sr$  doping,  $x^{eff} = 0.121$ .

## ACKNOWLEDGMENT

I thank Jun-Sik Lee for providing  $q_{cdw}$  data of  $La_{2-x}Sr_xCuO_4$  and for helpful correspondence.

- 
- <sup>1</sup> M. Bucher, “Superlattice origin of incommensurable density waves in  $La_{2-x}Ae_xCuO_4$  ( $Ae = Sr, Ba$ ),” arXiv:1308.1396v2
  - <sup>2</sup> M. Bucher, “Universality of density waves in  $p$ -doped  $La_2CuO_4$  and  $n$ -doped  $Nd_2CuO_{4+y}$ ” arXiv:1702.05364
  - <sup>3</sup> K. Yamada, C. H. Lee, K. Kurahashi, J. Wada, S. Wakimoto, S. Ueki, H. Kimura, Y. Endoh, S. Hosoya, G. Shirane, R. J. Birgeneau, M. Greven, M. A. Kastner, and Y. J. Kim, Phys. Rev. B **57**, 6165 (1998).
  - <sup>4</sup> J. M. Tranquada, B. J. Sternlieb, J. D. Axe, Y. Nakamura and S. Uchida, Nature **375**, 561 (1995).
  - <sup>5</sup> V. Thampy, X. M. Chen, Y. Cao, C. Mazzoli, A. M. Barbour, W. Hu, H. Miao, G. Fabbris, R. D. Zhong, G. D. Gu, J. M. Tranquada, I. K. Robinson, S. B. Wilkins, and M. P. M. Dean, Phys. Rev. B **95**, 241111(R) (2017).
  - <sup>6</sup> O. Ivashko, N. E. Shaik, X. Lu, C. G. Fatuzzo, M. Dantz, P. G. Freeman, D. E. McNally, D. Destraz, N. B. Christensen, T. Kurosawa, N. Momono, M. Oda, C. E. Matt, C. Monney, H. M. Ronnow, T. Schmitt, and J. Chang, Phys. Rev. B **95**, 214508 (2017).
  - <sup>7</sup> H. Miao, J. Lorenzana, G. Seibold, Y. Y. Peng, A. Amorese, F. Yakhou-Harris, K. Kummer, N. B. Brookes, R. M. Konik, V. Thampy, G. D. Gu, G. Ghiringhelli, L. Braicovich and M. P. M. Dean, Proc. Natl. Acad. Sci. **114**, 12430 (2017).
  - <sup>8</sup> H. Miao, R. Fumagalli, M. Rossi, J. Lorenzana, G. Seibold, F. Yakhou-Harris, K. Kummer, N. B. Brookes, G. D. Gu, L. Braicovich, G. Ghiringhelli and M. P. M. Dean, Phys. Rev. X **9**, 031042 (2019).
  - <sup>9</sup> Q. Wang, M. Horio, K. von Arx, Y. Shen, D. Mukkattukavil, Y. Sassa, O. Ivashko, C. E. Matt, S.

- Pyon, T. Takayama, H. Takagi, T. Kurosawa, N. Momono, M. Oda, T. Adachi, S. M. Haidar, Y. Koike, Y. Tseng, W. Zhang, J. Zhao, K. Kummer, M. Garcia-Fernandez, K. J. Zhou, N. B. Christensen, H. M. Rønnow, T. Schmitt and J. Chang, “High-Temperature Charge-Stripe Correlations in  $La_{1.675}Eu_{0.2}Sr_{0.125}CuO_4$ ,” arXiv:1912.00194v1
- <sup>10</sup> J.-J. Wen, H. Huang, S.-J. Lee, H. Jang, J. Knight, Y. S. Lee, M. Fujita, K. Suzuki, S. Asano, S. A. Kivelson, C.-C. Kao, and J.-S. Lee, *Nature Commun.* **10**, 3269 (2019).
- <sup>11</sup> H. Miao, G. Fabbris, C. S. Nelson, R. Acevedo-Esteves, Y. Li, G. D. Gu, T. Yilmaz, K. Kaznatcheev, E. Vescovo, M. Oda, K. Kurosawa, N. Momono, T. A. Assefa, I. K. Robinson, J. M. Tranquada, P. D. Johnson and M. P. M. Dean, “Discovery of Charge Density Waves in Cuprate Superconductors up to the Critical Doping and Beyond,” arXiv:2001.10294
- <sup>12</sup> J. Q. Lin, H. Miao, D. G. Mazzone, G. D. Gu, A. Nag, A. C. Walters, M. García-Fernández, A. Barbour, J. Pelliciani, I. Jarrige, M. Oda, K. Kurosawa, N. Momono, K. Zhou, V. Bisogni, X. Liu, and M. P. M. Dean, “Charge-density wave phonon induced softening in  $La_{2-x}Sr_xCuO_4$  cuprates driven by strong electronic correlations,” to appear in *Phys. Rev. Lett.* (2020).
- <sup>13</sup> J. M. Tranquada, J. D. Axe, N. Ichikawa, Y. Nakamura, S. Uchida, and B. Nachumi, *Phys. Rev. B* **54**, 7489 (1996).
- <sup>14</sup> J. M. Tranquada, J. D. Axe, N. Ichikawa, A. R. Moodenbaugh, Y. Nakamura, and S. Uchida, *Phys. Rev. Lett.* **78**, 338 (1997).
- <sup>15</sup> T. Niemöller, N. Ichikawa, T. Frello, H. Hünnefeld, N. H. Andersen, S. Uchida, J. R. Schneider and J. M. Tranquada, *Eur. Phys. J. B* **12**, 509 (1999).
- <sup>16</sup> M. v. Zimmermann, A. Vigliante, T. Niemöller, N. Ichikawa, T. Frello, J. Madsen, P. Wochner, S. Uchida, N. H. Andersen, and J. M. Tranquada, *Europhys. Lett.* **41**, 629 (1998).
- <sup>17</sup> J. Fink, E. Schierle, E. Weschke, J. Geck, D. Hawthorn, V. Soltwisch, H. Wadati, H.-H. Wu, H. A. Dürr, N. Wizen, B. Büchner, and G. A. Sawatzky, *Phys. Rev. B* **79**, 100502(R) (2009).
- <sup>18</sup> J. Fink, V. Soltwisch, J. Geck, E. Schierle, E. Weschke, and B. Büchner, *Phys. Rev. B* **83**, 092503 (2011).
- <sup>19</sup> A. J. Achkar, F. He, R. Sutarto, J. Geck, H. Zhang, Y.-J. Kim, and D. G. Hawthorn, *Phys. Rev. Lett.* **110**, 017001 (2013).
- <sup>20</sup> V. Thampy, M. P. M. Dean, N. B. Christensen, L. Steinke, Z. Islam, M. Oda, M. Ido, N. Momono, S. B. Wilkins, and J. P. Hill, *Phys. Rev. B* **90**, 100510(R) (2014).
- <sup>21</sup> N. B. Christensen, J. Chang, J. Larsen, M. Fujita, M. Oda, M. Ido, N. Momono, E. M. Forgan, A.

- T. Holmes, J. Mesot, M. Hücker, and M. v. Zimmermann, “Bulk charge stripe order competing with superconductivity in  $La_{1.88}Sr_{0.12}CuO_4$ ,” arXiv:1404.3192
- <sup>22</sup> X. M. Chen, V. Thampy, C. Mazzoli, A. M. Barbour, H. Miao, G. D. Gu, Y. Cao, J. M. Tranquada, M. P. M. Dean, and S. B. Wilkins, *Phys. Rev. Lett.* **117**, 167001 (2016).
- <sup>23</sup> H. Kimura, H. Goka, M. Fujita, Y. Noda, K. Yamada, and N. Ikeda, *Phys. Rev. B* **67**, 140503(R) (2003).
- <sup>24</sup> P. Abbamonte, A. Rusydi, S. Smadici, G. D. Gu, G. A. Sawatzky, and D. L. Feng, *Nature Phys.* **1**, 155 (2005).
- <sup>25</sup> Y. J. Kim, G. D. Gu, T. Gog, and D. Casa, *Phys. Rev. B* **77**, 064520 (2008).
- <sup>26</sup> J. Kim, H. Zhang, G. D. Gu, Y. J. Kim, *J. Supercond. Nov. Magn.* **22**, 251 (2009).
- <sup>27</sup> M. Hücker, M. v. Zimmermann, Z. J. Xu, J. S. Wen, G. D. Gu, and J. M. Tranquada, *Phys. Rev. B* **87**, 014501 (2013).
- <sup>28</sup> M. P. M. Dean, G. Dellea, M. Minola, S. B. Wilkins, R. M. Konik, G. D. Gu, M. Le Tacon, N. B. Brookes, F. Yakhov-Harris, K. Kummer, J. P. Hill, L. Braicovich, and G. Ghiringhelli, *Phys. Rev. B* **88**, 020403(R) (2013).
- <sup>29</sup> V. Thampy, S. Blanco-Canosa, M. García-Fernández, M. P. M. Dean, G. D. Gu, M. Först, T. Loew, B. Keimer, M. Le Tacon, S. B. Wilkins, and J. P. Hill, *Phys. Rev. B* **88**, 024505 (2013).
- <sup>30</sup> T. P. Croft, C. Lester, M. S. Senn, A. Bombardi, and S. M. Hayden, *Phys. Rev. B* **89**, 224513, (2014).
- <sup>31</sup> V. Khanna, R. Mankowsky, M. Petrich, H. Bromberger, S. A. Cavill, E. Möhr-Vorobeva, D. Nicoletti, Y. Laplace, G. D. Gu, J. P. Hill, M. Först, A. Cavalleri, and S. S. Dhesi, *Phys. Rev. B* **93**, 224522 (2016).
- <sup>32</sup> M. Fujita, K. Yamada, H. Hiraka, P. M. Gehring, S. H. Lee, S. Wakimoto, and G. Shirane, *Phys. Rev. B* **65**, 064505 (2002).
- <sup>33</sup> H. Matsushita, H. Kimura, M. Fujita, K. Yamada, K. Hirota, and Y. Endoh, *J. Phys. Chem. Solids* **60**, 1071 (1999).
- <sup>34</sup> M. Matsuda, M. Fujita, K. Yamada, R. J. Birgeneau, Y. Endoh, and G. Shirane, *Phys. Rev. B* **65**, 134515 (2002).
- <sup>35</sup> O. J. Lipscombe, S. M. Hayden, B. Vignolle, D. F. McMorrow, and T. G. Perring, *Phys. Rev. Lett.* **99**, 067002 (2007).
- <sup>36</sup> M. Matsuda, M. Fujita, S. Wakimoto, J. A. Fernandez-Baca, J. M. Tranquada, and K. Yamada,

- Phys. Rev. Lett. **101**, 197001 (2008).
- <sup>37</sup> M. Fujita, M. Enoki, and K. Yamada, J. Phys. Chem. Solids **69**, 3167 (2008).
- <sup>38</sup> A. T. Rømer, P. J. Ray, H. Jacobsen, L. Udby, B. M. Andersen, M. Bertelsen, S. L. Holm, N. B. Christensen, R. Toft-Petersen, M. Skoulatos, M. Laver, A. Schneidewind, P. Link, M. Oda, M. Ido, N. Momono, and K. Lefmann, Phys. Rev. B **91**, 174507 (2015).
- <sup>39</sup> H. Jacobsen, I. A. Zaliznyak, A. T. Savici, B. L. Winn, S. Chang, M. Hücker, G. D. Gu, and J. M. Tranquada, Phys. Rev. B **92**, 174525 (2015).
- <sup>40</sup> M. Fujita, H. Goka, K. Yamada, J. M. Tranquada, and L. P. Regnault, Phys. Rev. B **70**, 104517 (2004).
- <sup>41</sup> S. R. Dunsiger, Y. Zhao, Z. Yamani, W. J. L. Buyers, H. A. Dabkowska, and B. D. Gaulin, Phys. Rev. B **77**, 224410 (2008).
- <sup>42</sup> V. Balédent, B. Fauqué, Y. Sidis, N. B. Christensen, S. Pailhès, K. Conder, E. Pomjakushina, J. Mesot, and P. Bourges, Phys. Rev. Lett. **105**, 027004 (2010).
- <sup>43</sup> M. Hücker, M. v. Zimmermann, G. D. Gu, Z. J. Xu, J. S. Wen, G. Xu, H. J. Kang, A. Zheludev, and J. M. Tranquada, Phys. Rev. B **83**, 104506 (2011).
- <sup>44</sup> The data from Refs. 41 and 43 were used with a *Ba* concentration re-calibrated according to Ref. 43.
- <sup>45</sup> Z. Xu, C. Stock, S. Chi, A. I. Kolesnikov, G. Xu, G. Gu, and J. M. Tranquada, Phys. Rev. Lett. **113**, 177002 (2014).
- <sup>46</sup> V. Bochko and Z. K. Silagadze, “On the electrostatic potential and electric field of a uniformly charged disk,” arXiv:2004.04540
- <sup>47</sup> J. D. Axe, A. H. Moudden, D. Hohlwein, D. E. Cox, K. M. Mohanty, A. R. Moodenbaugh, and Y. Xu, Phys. Rev. Lett. **62**, 2751 (1989).
- <sup>48</sup> P. G. Radaelli, D. G. Hinks, A. W. Mitchell, B. A. Hunter, J. L. Wagner, B. Dabrowski, K. G. Vandervoort, H. K. Viswanathan, and J. D. Jorgensen, Phys. Rev. B **49**, 4163 (1994).
- <sup>49</sup> G. Ghiringhelli, M. Le Tacon, M. Minola, S. Blanco-Canosa, C. Mazzoli, N. B. Brookes, G. M. De Luca, A. Frano, D. G. Hawthorn, F. He, T. Loew, M. Moretti Sala, D. C. Peets, M. Salluzzo, E. Schierle, R. Sutarto, G. A. Sawatzky, E. Weschke, B. Keimer, and L. Braicovich, Science, **337**, 821 (2012).
- <sup>50</sup> J. Chang, E. Blackburn, A. T. Holmes, N. B. Christensen, J. Larsen, J. Mesot, R. Liang, D. A. Bonn, W. N. Hardy, A. Watenphul, M. v. Zimmermann, E. M. Forgan, and S. M. Hayden,

- Nat. Phys. **8**, 871 (2012).
- <sup>51</sup> H.-H. Wu, M. Buchholz, C. Trabant, C. F. Chang, A. C. Komarek, F. Heig, M. v. Zimmermann, M. Cwik, F. Nakamura, M. Braden, and C. Schüßler-Langeheine, Nat. Commun. **3**, 1023 (2012).
- <sup>52</sup> M.-H. Julien, Physica B **329-333**, 693 (2003).
- <sup>53</sup> M. Hücker, M. v. Zimmermann, Z. J. Xu J. S. Wen G. D. Gu, and J. M. Tranquada, Phys. Rev. B **87**, 014501 (2013).
- <sup>54</sup> J. J. Wagman, G. Van Gastel, K. A. Ross, Z. Yamani, Y. Zhao, Y. Qiu, J. R. D. Copley, A. B. Kallin, E. Mazurek, J. P. Carlo, H. A. Dabkowska, and B. D. Gaulin, Phys. Rev. B **88**, 014412 (2013).
- <sup>55</sup> D. Vaknin, S. K. Sinha, D. E. Moncton, D. C. Johnston, J. M. Newsam, C. R. Safinya, and H. E. King, Jr., Phys. Rev. Lett. **58**, 2802 (1987).
- <sup>56</sup> K. Yamada, E. Kudo, Y. Endoh, Y. Hidaka, M. Oda, M. Suzuki, and T. Murakami, Solid State Commun. **64**, 753 (1987).
- <sup>57</sup> K. Yamada, K. Kakurai, Y. Endoh, T. R. Thurston, M. A. Kastner, R. J. Birgeneau, G. Shirane, Y. Hidaka, and T. Murakami, Phys. Rev. B **40**, 4557 (1989).
- <sup>58</sup> F. Coneri, S. Sanna, K. Zheng, J. Lord, and R. De Renzi, Phys. Rev. B **81**, 104507 (2010).
- <sup>59</sup> N. S. Headings, S. M. Hayden, R. Coldea, and T. G. Perring Phys. Rev. Lett. **105**, 247001 (2010).
- <sup>60</sup> J. M. Tranquada, G. Xu, and I. A. Zaliznyak, J. Magn. Magn. Mat. **350**, 148 (2014).